Deciphering the universal scaling of particle transverse momentum spectra in heavy-ion collisions

Xi-Yao Guo,[1] Hua Zheng,[1,*] Wen-Chao Zhang,[1] Li-Lin Zhu,[2] Xing-Quan Liu,[3] Zhi-Guang Tan,[4] Dai-Mei Zhou,[5] and Ben-Hao Sa[5,6]

[1]*School of Physics and Information Technology, Shaanxi Normal University, Xi'an 710119, China*

[2]*College of Physics, Sichuan University, Chengdu 610064, China*

[3]*Key Laboratory of Radiation Physics and Technology of the Ministry of Education, Institute of Nuclear Science and Technology, Sichuan University, Chengdu 610064, China*

[4]*School of Electronic Information and Electrical Engineering, Changsha University, Changsha 410003, China*

[5]*Key Laboratory of Quark Lepton Physics (MOE) and Institute of Particle Physics, Central China Normal University, Wuhan 430079, China*

[6]*China Institute of Atomic Energy, P.O. Box 275 (10), Beijing 102413, China*

(Received 20 April 2026; revised 6 June 2026; accepted 8 July 2026; published 3 August 2026)

We systematically investigate the scaling properties of the transverse momentum spectra for pions, kaons, and protons in Au + Au collisions at $\sqrt{s_{NN}} = 7.7$, 11.5, 14.5, 19.6, 27, 39, 62.4, and 200 GeV, as well as in U + U collisions at $\sqrt{s_{NN}} = 193$ GeV, across different centrality classes, using experimental data from the collaborations at the Relativistic Heavy Ion Collider (RHIC). Universal scaling emerges when the particle transverse momentum spectra are scaled by global physical quantities, i.e., the average total particle multiplicity and mean transverse momentum, confirming recent scaling findings from the data at the Large Hadron Collider (LHC) by the ExTrEMe Collaboration. The scaling behavior breaks down in the high p_T region and in peripheral collisions. We provide a natural explanation for these observations in the framework of a blast-wave-type model built upon the Cooper-Frye formula. Furthermore, we demonstrate the equivalence between the scaling found by the ExTrEMe Collaboration and the Hwa-Yang scaling, which was proposed two decades ago.

DOI: 10.1103/2dp4-q43h

I. INTRODUCTION

The primary goal of high energy collision experiments in terrestrial laboratories is to explore the fundamental properties of nuclear matter under extreme conditions, i.e., high temperature and density [1–7]. Since the collision processes cannot be measured directly, experimental observables measured from the final-state particles act as essential probes to decipher their properties and dynamical evolution [8–14]. Among these observables, the transverse momentum p_T spectra of identified particles are useful for investigating particle collective dynamics and hadronization mechanisms in high energy heavy-ion collisions [15–20]. Measurements at the Relativistic Heavy Ion Collider (RHIC) and the Large Hadron Collider (LHC) have revealed a range of striking phenomena from particle transverse momentum spectra, such as the anomalous enhancement of baryon production at intermediate transverse momentum region [21–23], strong high-p_T suppression of hadrons [24,25], and the number-of-constituent-quark (NCQ) scaling of elliptic flow of identified particles [26–30]. These observations provide key insights into the properties and hadronization mechanisms of the strongly coupled quark-gluon plasma (QGP).

Among various approaches to studying heavy-ion collision physics, the search for universal scaling patterns in observables plays an important role. Scaling simply implies that a universal physics exists and can deepen our understanding, such as Koba-Nielsen-Olesen (KNO) scaling [31–33], Bjorken scaling [34,35], Regge scaling [36–38], and Feynman scaling [39–41]. The scaling behavior of particle transverse momentum spectra has long served as a valuable probe in relativistic heavy-ion collisions [42–45]. In 2003, Hwa and Yang discovered pion transverse momentum spectra scaling, now known as Hwa-Yang scaling, in heavy-ion collisions across different collision energies and centralities by introducing a scaling variable $z = p_T/K$, where K is a parameter that depends on the centrality and collision energy [43–45]. They further showed that this scaling behavior could be used to define a KNO-like scaling function $\Psi(u)$ with $u = p_T/\langle p_T \rangle$, which removes the dependence on the scaling parameter and relies only on the global quantity, i.e., the mean transverse momentum $\langle p_T \rangle$. This approach was later extended to various collision systems, particle species, and collision energies, establishing a comprehensive scaling framework, which is interpreted within the color string percolation model [46–55]. It was concluded that the scaling is universal, independent of collision energies, collision

*Contact author: zhengh@snnu.edu.cn

Published by the American Physical Society under the terms of the Creative Commons Attribution 4.0 International license. Further distribution of this work must maintain attribution to the author(s) and the published article's title, journal citation, and DOI. Funded by SCOAP³.

systems, and particle species. Recently, a new particle transverse momentum spectra scaling was proposed in Refs. [56–59]. The variable $x_T = p_T/\langle p_T\rangle$ and a scaled spectrum $U(x_T) = (\langle p_T\rangle/N)dN/dp_T$, which are scaled using the global physical quantities of the average total particle multiplicity N for the chosen particle species and mean transverse momentum $\langle p_T\rangle$, are adopted. $U(x_T)$ for pions at the LHC exhibits a nearly universal, centrality-independent scaling. Such behavior has also been observed in the hybrid hydrodynamic simulations and interpreted as a possible signature of hydrodynamic evolution [56]. Similar universal scalings are also found for kaons, and protons at the LHC [57–59]. Furthermore, a comprehensive study reveals that the hybrid hydrodynamic models have little flexibility in describing the scaled spectrum observables by varying the model parameters [59]. Therefore, the underlying physical mechanism leading to such scaling remains unclear.

It is natural to extend this particle transverse momentum spectra scaling search to the pion, kaon, and proton spectra in heavy-ion collisions at the RHIC, as motivated by the Hwa-Yang scaling. It is expected that the scaling is universal as well. In this paper, the scaling properties of the transverse momentum spectra for pions, kaons, and protons in Au + Au collisions at $\sqrt{s_{NN}} = 7.7$, 11.5, 14.5, 19.6, 27, 39, 62.4, and 200 GeV, as well as in U + U collisions at $\sqrt{s_{NN}} = 193$ GeV at the RHIC are investigated. We demonstrate that the observed scaling persists across this wide energy range and centrality classes at both the RHIC and LHC, and provide a natural theoretical interpretation in the framework of a blast-wave-type model built upon the Cooper-Frye formula with certain assumptions. Furthermore, we establish the relation between the scaling found by the ExTrEMe Collaboration and the Hwa-Yang scaling, demonstrating their equivalence and deepening our understanding of the particle spectra scaling found in heavy-ion collisions.

The organization of this paper is as follows. In Sec. II, we briefly describe the procedure for searching for particle transverse momentum spectra scaling. Section III presents the scalings of the transverse momentum spectra for pions, kaons, and protons in Au + Au collisions at RHIC energies from 7.7 to 200 GeV and in U + U collisions at 193 GeV. A comparison with the results obtained at the LHC is also shown. In Sec. IV, we give our explanation for the mechanism leading to the particle transverse momentum spectra scaling in the framework of a blast-wave-type model built upon the Cooper-Frye formula, showing quantitative agreement with data. We also explicitly demonstrate the equivalence between the scaling found by the ExTrEMe Collaboration and the Hwa-Yang scaling. Finally, a brief conclusion is given in Sec. V.

II. METHOD TO SEARCH FOR THE PARTICLE TRANSVERSE MOMENTUM SPECTRA SCALING

As done in Refs. [56–59], the experimental data of particle transverse momentum spectra are converted into the transverse momentum differential distribution dN/dp_T. In order to scale the particle distribution, the average total particle multiplicity N and mean transverse momentum $\langle p_T\rangle$ of a given particle species are required for a given centrality. Note that they are calculated from dN/dp_T starting from $p_T = 0$ GeV/c. With N and $\langle p_T\rangle$ for each centrality, the scaled transverse momentum distribution

$$U(x_T) = \frac{\langle p_T\rangle}{N}\frac{dN}{dp_T} = \frac{1}{N}\frac{dN}{dx_T} \tag{1}$$

can be derived, where $x_T = p_T/\langle p_T\rangle$. The uncertainties of the scaled transverse momentum distribution $U(x_T)$ are estimated from the particle p_T spectrum errors, as well as the uncertainties of $\langle p_T\rangle$ and N.

Then the scaled particle transverse momentum spectra $U(x_T)$ as function of x_T for all centralities are plotted together. If all scaled data points collapse onto a single curve, it means that the particle transverse momentum spectra scaling exists. Usually, the scaling is not perfect. The ratio

$$R_i(x_T) = \frac{U_i(x_T)}{U_{MCC}(x_T)} \tag{2}$$

is defined to quantify any deviations, where $U_i(x_T)$ is the scaled spectrum for the ith centrality bin, and $U_{MCC}(x_T)$ corresponds to scaled spectrum for the most central centrality (MCC). Since different centrality classes have different $\langle p_T\rangle$ values and thus different x_T, we interpolate the scaled spectrum $U_{MCC}(x_T)$ onto the x_T points of each centrality bin for a point-by-point comparison. The same approach was applied in Ref. [56] to ensure a consistent quantitative evaluation of scaling violations across centralities.

III. RESULTS OF PION, KAON, AND PROTON TRANSVERSE MOMENTUM SPECTRA SCALINGS AT RHIC

The STAR and PHENIX Collaborations at RHIC have published data for the transverse momentum spectra of pions, kaons, and protons at midrapidity across different centralities, the values of dN/dy and $\langle p_T\rangle$ along with the systematic uncertainties at the same time [60,61,63,64]. Therefore we can directly collect the data from Au + Au collisions at $\sqrt{s_{NN}} = 7.7$ [60], 11.5 [60], 14.5 [61], 19.6 [60], 27 [60], 39 [60], and 200 [63] GeV as well as from U + U collisions at $\sqrt{s_{NN}} = 193$ [64] GeV, and conduct the analyses. For Au + Au collisions at $\sqrt{s_{NN}} = 62.4$ GeV [62], only the particle p_T spectra data are available, so we fit the particle p_T spectrum well using a combined fit with a Bose-Einstein function and an m_T-exponential function and perform the extrapolation. Then the corresponding dN/dy and $\langle p_T\rangle$ are evaluated. Unlike how the systematic uncertainties of the experimental data for dN/dy and $\langle p_T\rangle$ were determined, the systematic uncertainties of dN/dy and $\langle p_T\rangle$ at 62.4 GeV are assigned based on the typical values reported in the STAR analyses [60,61,64], i.e., about 10% for dN/dy and 5% for $\langle p_T\rangle$. The scaled transverse momentum spectra $U(x_T)$, following the procedure in Sec. II, for pions, kaons, and protons across collision centralities, systems and energies at RHIC are presented in Figs. 1–3, respectively. The results are shown in the same pattern. For a given collision energy, the scaled data points $U(x_T)$ corresponding

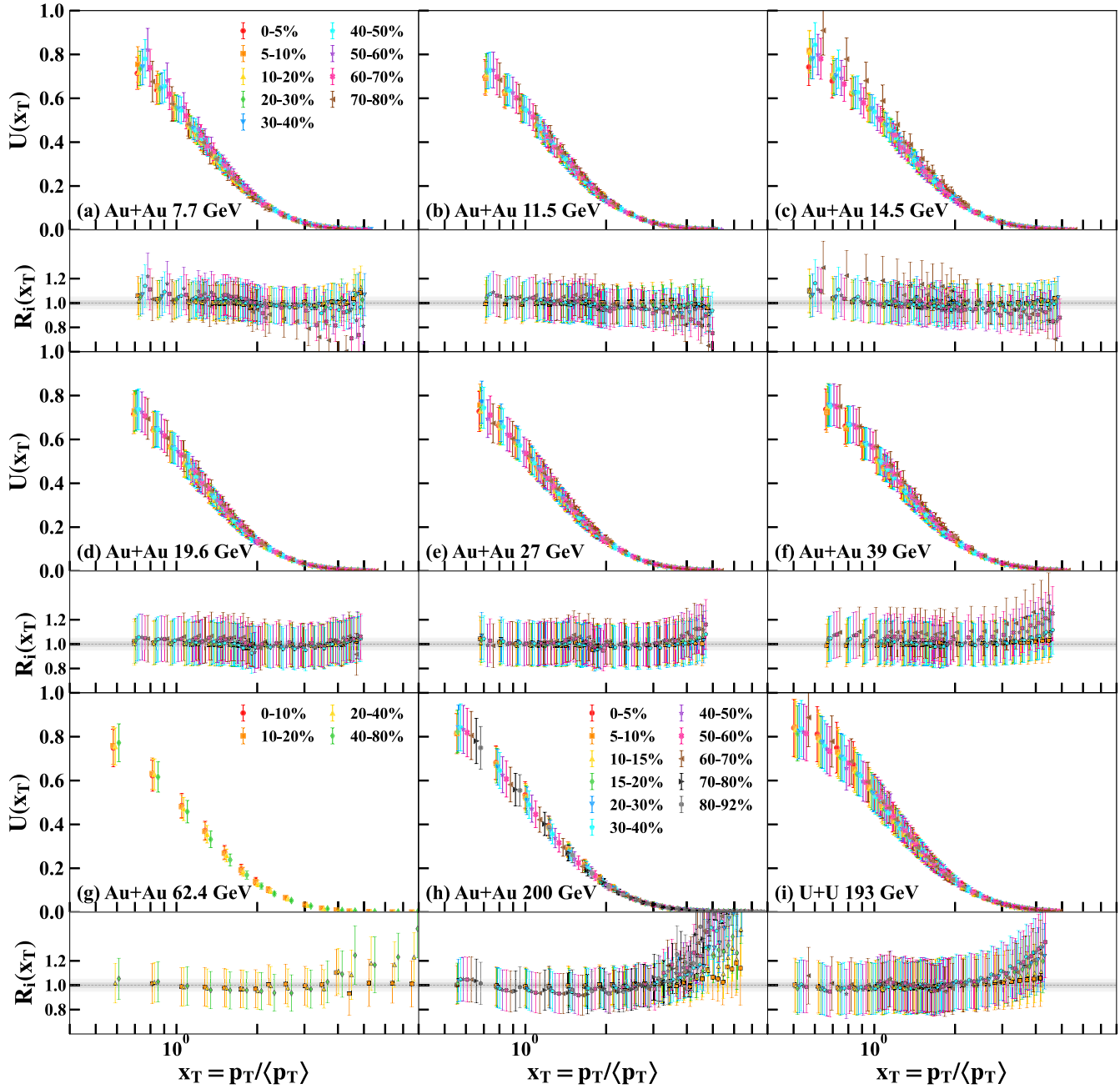


FIG. 1. For each row, the top panel shows the scaled spectra $U(x_{\mathrm{T}})$ for π^+ in Au + Au collisions at 7.7 [60], 11.5 [60], 14.5 [61], 19.6 [60], 27 [60], 39 [60], 62.4 [62], and 200 [63] GeV, as well as in U + U collisions at 193 [64] GeV, respectively. The bottom panel shows the corresponding ratios between $U_i(x_{\mathrm{T}})$ from the ith centrality bin and that for the most central collisions in Au + Au collisions at 7.7–200 GeV and in U + U collisions at 193 GeV. The most central centrality is 0–5% for all the collision systems except that it is 0–10% in Au + Au collisions at 62.4 GeV.

to different centralities are distinguished by distinct colors and markers, shown in the top panel. Error bars represent the estimated uncertainties. To visualize the quality of the particle spectra scaling across the entire centrality range, the ratios $R_i(x_{\mathrm{T}})$, Eq. (2), are also shown in the bottom panel. The scaled spectra $U(x_{\mathrm{T}})$ for pions across RHIC energies are shown in Fig. 1. The scaled data points collapse onto a single curve at a given collision energy, revealing a particle transverse momentum spectra scaling independent of centrality and confirming the scaling findings at the LHC [56,57]. Note that some deviations are observed in peripheral Au + Au collisions at $\sqrt{s_{NN}} = 14.5$ GeV. The ratios $R_i(x_{\mathrm{T}})$ reveal more details at high p_{T} that the scaling quality is not as good as that at low p_{T}. This behavior is attributed to the transition to a (semi)hard physics regime beyond hydrodynamics. Overall, a consistent pattern is observed across the RHIC energies. Similar results are found for kaons and protons, as shown in Figs. 2 and 3.

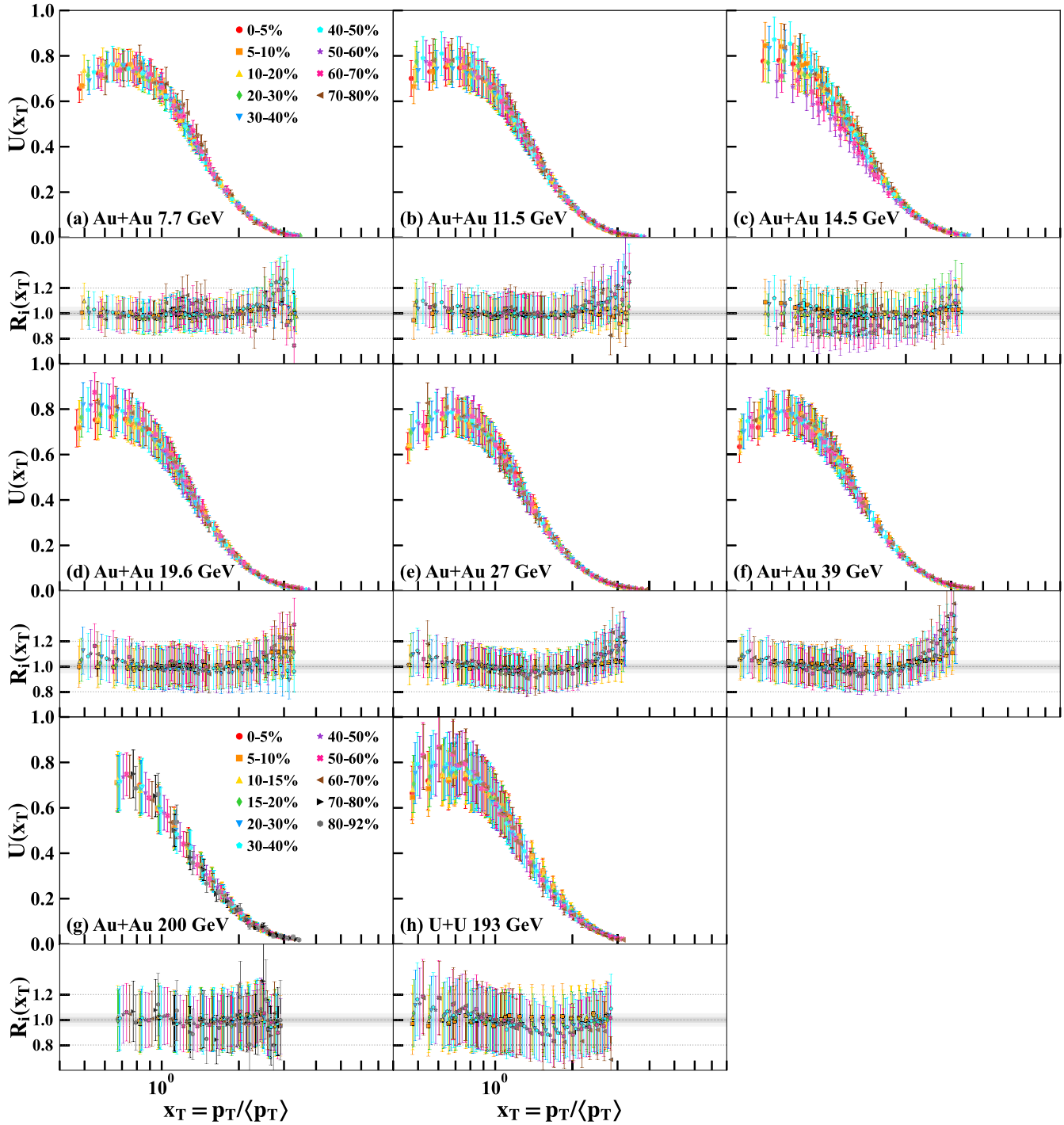


FIG. 2. For each row, the top panel shows the scaled spectra $U(x_{\mathrm{T}})$ for K^+ in Au + Au collisions at 7.7 [60], 11.5 [60], 14.5 [61], 19.6 [60], 27 [60], 39 [60], and 200 [63] GeV, as well as in U + U collisions at 193 [64] GeV. The bottom panel shows the corresponding ratios between $U_i(x_{\mathrm{T}})$ from the ith centrality bin and that for the most central collisions in Au + Au collisions at 7.7–200 GeV and in U + U collisions at 193 GeV. The most central centrality is 0–5% for all the collision systems.

A closer quantitative comparison among the particle species reveals subtle differences. The scaled spectra for pions adhere most precisely to the universal curve across all centralities, while kaons and protons show systematically larger deviations in peripheral collisions. This mass hierarchy, where heavier hadrons show relatively worse scaling, is consistent with phenomena observed at the LHC [57] and can be understood within the collective expansion framework. In peripheral collisions, where radial flow is weaker, mass-dependent modifications of particle spectra become

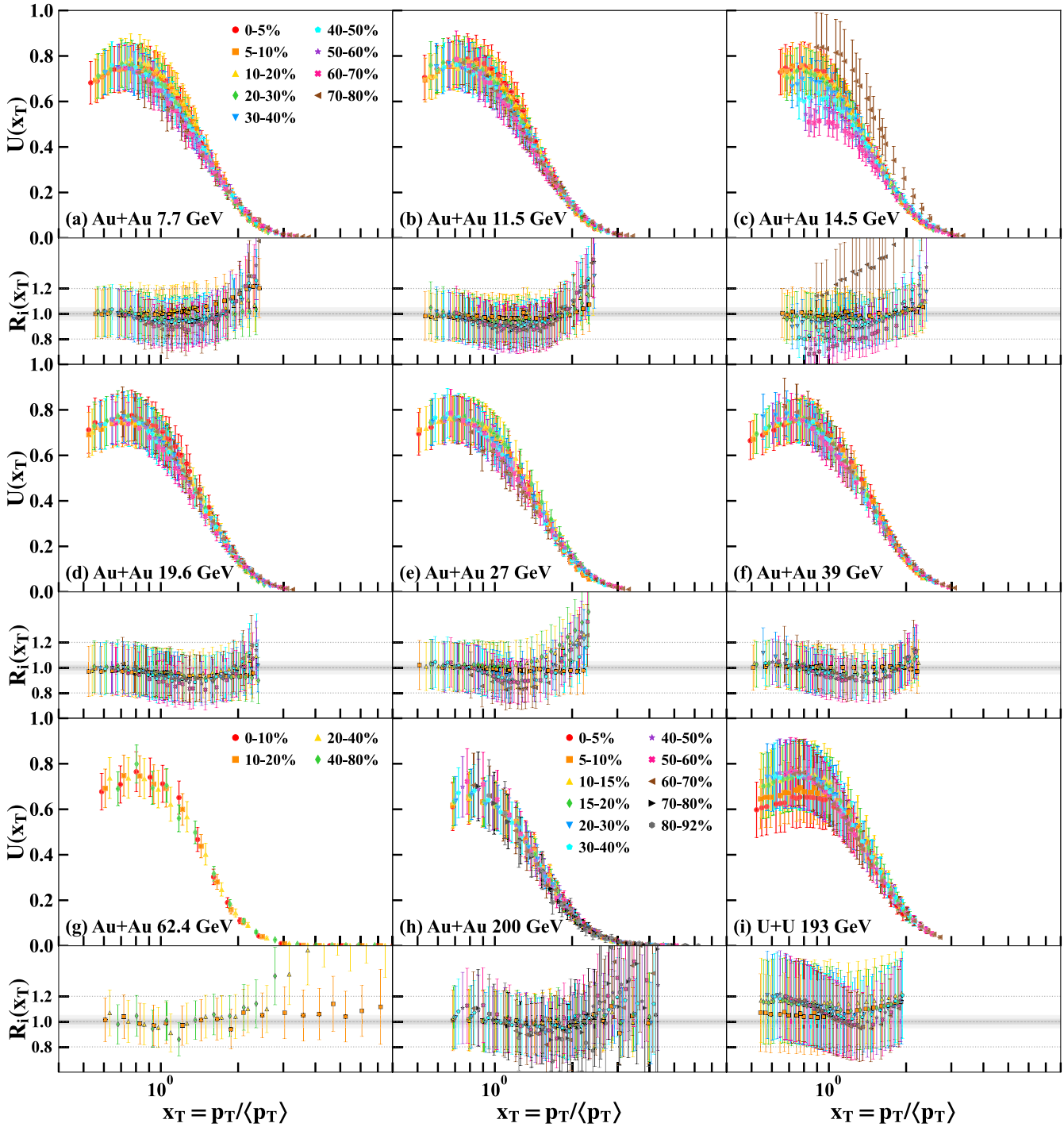


FIG. 3. For each row, the top panel shows the scaled spectra $U(x_{\mathrm{T}})$ for p in Au + Au collisions at 7.7 [60], 11.5 [60], 14.5 [61], 19.6 [60], 27 [60], 39 [60], 62.4 [62], and 200 [63] GeV, as well as U + U collisions at 193 [64] GeV. The bottom panel shows the corresponding ratios between $U_i(x_{\mathrm{T}})$ from the ith centrality bin and that for the most central collisions in Au + Au collisions at 7.7–200 GeV and in U + U collisions at 193 GeV. The most central centrality is 0-5% for all the collision systems except that it is 0–10% in Au + Au collisions at 62.4 GeV.

more apparent compared to central collisions. Consequently, heavier particles deviate more noticeably from the scaling in peripheral collisions [42,65].

We further investigate whether this scaling is universal and independent of the collision energy. Figure 4 shows the scaled spectra $U(x_{\mathrm{T}})$ for the same centrality interval (0–40%) for different collision energies, including the results from LHC [56]. It is observed that the data points from 7.7 to 200 GeV collapse onto a single curve, demonstrating the universality of this scaling. The persistence of scaling from 7.7 to 200 GeV

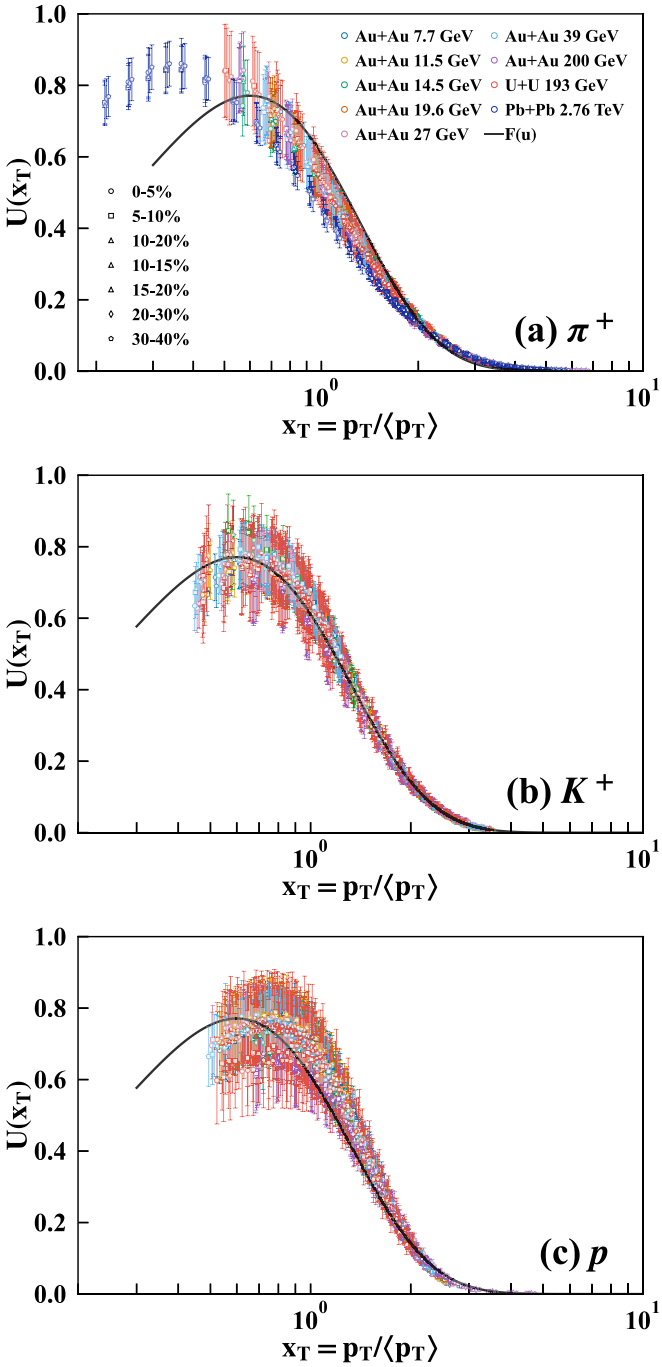


FIG. 4. (a) The scaled spectra $U(x_{\mathrm{T}})$ for π^+ in centrality interval 0–40%, including the Au + Au collisions at $\sqrt{s_{NN}} = 7.7$–200 GeV, U + U collisions at 193 GeV, and Pb + Pb collisions at 2.76 TeV. (b), (c) The scaled spectra $U(x_{\mathrm{T}})$ for K^+ and p in Au + Au and U + U collisions at RHIC energies. The curves shown in panels (a)–(c) are the same and correspond to Eq. (27).

in Au + Au and U + U collisions, as well as the results from the LHC [56], establishes the scaled spectra as a baseline. Any clear deviation from the observed scaling could serve as a signal of different physics processes at the RHIC and LHC [56].

IV. DISCUSSIONS

It has been shown that the particle spectra scaling exists and is independent of collision energies, collision centralities, and particle species. The ExTrEMe Collaboration has demonstrated through event-by-event hybrid hydrodynamic simulations that this scaling phenomenon is naturally reproduced in fluid-dynamical models [56–59]. It was suggested that this scaling can serve as a probe of collective dynamics in heavy-ion collisions. However, a comprehensive study reveals that the hybrid hydrodynamic models have little flexibility in describing the scaled spectrum observables by varying the model parameters [59]. This inspires us to pursue the origin of this universal scaling.

The hydrodynamic description provides a state-of-the-art framework for understanding collective expansion in heavy-ion collisions [13,66–70]. The produced matter is treated as a strongly coupled fluid that expands and cools in a hydrodynamic model. The dynamics of the system is governed by the conservation of energy and momentum, with transport coefficients such as shear and bulk viscosity accounting for dissipative effects. At late times, when the temperature becomes lower than the critical temperature, particles freeze out via the Cooper-Frye prescription.

The Cooper-Frye formula is written as [71–75]

$$E\frac{d^3N}{dp^3} = \int_{\Sigma^\mu} d^3\sigma_\mu p^\mu f(x,p), \tag{3}$$

where Σ^μ is the freeze-out hypersurface and σ_μ is its covariant normal vector. $f(x,p)$ is the Lorentz-invariant Boltzmann distribution at the kinetic freeze-out temperature T_K, given by [4,76]

$$f(x,p) = \frac{g\xi}{(2\pi)^3}\exp\left(-\frac{p^\mu u_\mu}{T_K}\right). \tag{4}$$

Here, g is the degeneracy factor and ξ is the fugacity for the particle. The four-momentum p^μ takes the form

$$\begin{aligned} p^\mu &= (e,\boldsymbol{p}) = (e,\boldsymbol{p}_{\mathrm{T}},p_z) \\ &= (m_{\mathrm{T}}\cosh y,\ p_{\mathrm{T}}\cos\phi_p,\ p_{\mathrm{T}}\sin\phi_p,\ m_{\mathrm{T}}\sinh y), \end{aligned} \tag{5}$$

while the flow four-velocity $u^\mu(x)$ is

$$\begin{aligned} u^\mu &= \gamma_{\mathrm{T}}(\cosh\eta,\boldsymbol{\beta},\sinh\eta) \\ &= \cosh\rho(\cosh\eta,\ \tanh\rho\cos\phi_b,\ \tanh\rho\sin\phi_b,\ \sinh\eta), \end{aligned} \tag{6}$$

with $\boldsymbol{\beta}$ the transverse flow velocity. The angles ϕ_p and ϕ_b correspond, respectively, to the azimuthal angles of the particle momentum and the transverse flow velocity relative to the x axis. $p^\mu u_\mu$ can be read as [74,77]

$$\begin{aligned} p^\mu u_\mu &= \gamma_{\mathrm{T}}(e\cosh\eta - \boldsymbol{p}_{\mathrm{T}}\cdot\boldsymbol{\beta} - p_z\sinh\eta), \\ &= m_{\mathrm{T}}\cosh\rho\cosh(\eta-y) - p_{\mathrm{T}}\sinh\rho\cos(\phi_p-\phi_b). \end{aligned} \tag{7}$$

Under the assumption that Σ^μ is a constant-proper-time surface $\tau = \text{const}$, the normal element takes the explicit form

$$d^3\sigma_\mu = (\cosh\eta,\ 0,\ 0,\ -\sinh\eta)\tau r\, dr d\eta d\phi_b. \tag{8}$$

Therefore we obtain

$$p^\mu d^3\sigma_\mu = \tau m_{\rm T}\cosh(\eta - y) d\eta r dr d\phi_b. \tag{9}$$

Substituting the expressions for $p^\mu d^3\sigma_\mu$, $f(x,p)$, and $p^\mu u_\mu$ into the Cooper-Frye formula Eq. (3) gives

$$E\frac{d^3N}{dp^3} = \frac{g\xi}{(2\pi)^3}\int \tau r dr d\eta d\phi_b\, m_{\rm T}\cosh(\eta - y) \times \exp\left[-\frac{m_{\rm T}\cosh\rho\cosh(\eta - y)}{T_K} + \frac{p_{\rm T}\sinh\rho}{T_K}\cos(\phi_p - \phi_b)\right]. \tag{10}$$

The integral yields the modified Bessel function I_0 [74,77]

$$\int_0^{2\pi}\exp\left[\frac{p_{\rm T}\sinh\rho}{T_K}\cos(\phi_p - \phi_b)\right]d\phi_b = 2\pi I_0\left(\frac{p_{\rm T}\sinh\rho}{T_K}\right). \tag{11}$$

Substituting Eq. (11) into Eq. (10) and simplifying the prefactor, we obtain the invariant particle spectrum

$$E\frac{d^3N}{dp^3} = \frac{g\xi}{(2\pi)^2}\int \tau r dr d\eta\, m_{\rm T}\cosh(\eta - y) \times e^{-m_{\rm T}\cosh\rho\cosh(\eta - y)/T_K} I_0\left(\frac{p_{\rm T}\sinh\rho}{T_K}\right). \tag{12}$$

Using the relation $E\frac{d^3N}{dp^3} = \frac{d^2N}{2\pi p_{\rm T} dp_{\rm T} dy}$, one has

$$\frac{d^2N}{2\pi p_{\rm T} dp_{\rm T} dy} = \frac{g\xi}{(2\pi)^2}\int \tau r dr d\eta\, m_{\rm T}\cosh(\eta - y) \times e^{-m_{\rm T}\cosh\rho\cosh(\eta - y)/T_K} I_0\left(\frac{p_{\rm T}\sinh\rho}{T_K}\right). \tag{13}$$

At midrapidity ($y \approx 0$), we take the approximation that the main contribution is from $\eta \approx y$ and have $\cosh(\eta - y) = 1$. We also take the assumption that the transverse flow rapidity ρ is independent of the radial coordinate r. Therefore, one has

$$\left.\frac{d^2N}{2\pi p_{\rm T} dp_{\rm T} dy}\right|_{y=0} = \frac{g\xi}{8\pi^2}\tau\Delta\eta R^2 m_{\rm T} \times e^{-m_{\rm T}\cosh\rho/T_K} I_0\left(\frac{p_{\rm T}\sinh\rho}{T_K}\right). \tag{14}$$

$\Delta\eta$ is a constant to take into count the contribution from η space. Its value does not change our conclusion and will be shown in the following. In the midrapidity region, the rapidity dependence of the particle spectrum is very weak, thus the single differential particle spectrum is

$$\frac{dN}{dp_{\rm T}} = \frac{g\xi}{4\pi}\tau\Delta\eta\Delta y R^2 p_{\rm T} m_{\rm T} e^{-m_{\rm T}\cosh\rho/T_K} I_0\left(\frac{p_{\rm T}\sinh\rho}{T_K}\right), \tag{15}$$

where Δy is the midrapidity width.

To obtain analytic formula for deciphering the origin of particle transverse momentum spectra scaling, we take the massless particle limit and have $m_{\rm T} \approx p_{\rm T}$. Therefore

$$\frac{dN}{dp_{\rm T}} \approx \frac{g\xi}{4\pi}\tau\Delta\eta\Delta y R^2 p_{\rm T}^2 e^{-p_{\rm T}\cosh\rho/T_K} I_0\left(\frac{p_{\rm T}\sinh\rho}{T_K}\right). \tag{16}$$

Using the asymptotic approximation $I_0(z) \approx e^z/\sqrt{2\pi z}$ for $z \equiv p_{\rm T}\sinh\rho/T_K$, which is justified for the majority of experimental data points, we obtain

$$\frac{dN}{dp_{\rm T}} \approx \frac{g\xi}{4\pi}\tau\Delta\eta\Delta y R^2 \frac{p_{\rm T}^{3/2}}{\sqrt{2\pi\sinh\rho/T_K}} \times \exp\left[-\frac{p_{\rm T}(\cosh\rho - \sinh\rho)}{T_K}\right]. \tag{17}$$

Defining an effective temperature

$$T_{\rm eff} \equiv \frac{T_K}{\cosh\rho - \sinh\rho} = T_K e^\rho, \tag{18}$$

the expression of $\frac{dN}{dp_{\rm T}}$ simplifies to

$$\frac{dN}{dp_{\rm T}} = C_0\, p_{\rm T}^{3/2}\, e^{-p_{\rm T}/T_{\rm eff}}, \tag{19}$$

where $C_0 = \frac{g\xi}{4\pi}\tau\Delta\eta\Delta y R^2 \frac{1}{\sqrt{2\pi\sinh\rho/T_K}}$ is a constant.

Now we can calculate the mean transverse momentum $\langle p_{\rm T}\rangle$ and average total multiplicity N for a given particle. The mean transverse momentum is

$$\langle p_{\rm T}\rangle = \frac{\int_0^\infty p_{\rm T}\frac{dN}{dp_{\rm T}}dp_{\rm T}}{\int_0^\infty \frac{dN}{dp_{\rm T}}dp_{\rm T}} = \frac{\int_0^\infty p_{\rm T}^{5/2}e^{-p_{\rm T}/T_{\rm eff}}dp_{\rm T}}{\int_0^\infty p_{\rm T}^{3/2}e^{-p_{\rm T}/T_{\rm eff}}dp_{\rm T}} = \frac{T_{\rm eff}^{7/2}\Gamma(7/2)}{T_{\rm eff}^{5/2}\Gamma(5/2)} = \frac{5}{2}T_{\rm eff}. \tag{20}$$

Therefore, the relation between $\langle p_{\rm T}\rangle$ and effective temperature $T_{\rm eff}$ is

$$T_{\rm eff} = \frac{2}{5}\langle p_{\rm T}\rangle. \tag{21}$$

Similarly, the average total multiplicity is

$$N = \int_0^\infty \frac{dN}{dp_{\rm T}}dp_{\rm T} = C_0\int_0^\infty p_{\rm T}^{3/2}e^{-p_{\rm T}/T_{\rm eff}}dp_{\rm T}. \tag{22}$$

Using the relation Eq. (21) and introducing the scaled variable $u = p_{\rm T}/\langle p_{\rm T}\rangle$, we obtain

$$N = C_0\langle p_{\rm T}\rangle^{5/2}\int_0^\infty u^{3/2}e^{-5u/2}du. \tag{23}$$

C_0 can be expressed as

$$C_0 = \frac{N}{\langle p_{\rm T}\rangle^{5/2}}\frac{25}{3}\sqrt{\frac{5}{2\pi}}. \tag{24}$$

Substituting C_0 into Eq. (19), one obtains

$$\frac{dN}{dp_{\rm T}} = \frac{N}{\langle p_{\rm T}\rangle}\frac{25}{3}\sqrt{\frac{5}{2\pi}}\,u^{3/2}e^{-5u/2}. \tag{25}$$

Thus the scaled particle transverse momentum spectrum is

$$U(x_{\rm T}) = \frac{\langle p_{\rm T}\rangle}{N}\frac{dN}{dp_{\rm T}} = F(u), \tag{26}$$

where the scaling function $F(u)$ is

$$F(u) = \frac{25}{3}\sqrt{\frac{5}{2\pi}}\,u^{3/2}e^{-5u/2}. \tag{27}$$

Equation (27) does not depend on the collision centralities, collision energies, and collision systems. Therefore, the universal scaling behavior observed from particle transverse momentum spectra in heavy-ion collisions can be naturally understood in the framework of the blast-wave-type model built upon the Cooper-Frye formula with the assumptions made in the derivation. It is not surprising to see that the particle transverse momentum spectra scaling has the particle mass dependence from data [56–59] since we take the massless particle limit. In Fig. 4, the curves from Eq. (27) are also shown, which can describe the general features of the particle transverse momentum spectra scaling from experimental data. It is interesting already since the model is so simple. We note that a clear deviation from the universal scaling curve is observed in Fig. 4(a) in the low $x_{\rm T}$ region ($x_{\rm T} < 0.5$). It may be caused by our assumptions. The reason for this deviation is out of the scope of the present paper. Equation (27) may also explain why the hybrid hydrodynamic models have little flexibility in describing the scaled spectrum observables by varying model parameters. Because the universal scaling may be strongly relevant to the Cooper-Frye formula which is used for the particle freeze-out in hydrodynamic model. Our conjecture is strongly intuitive, but it is worth investigating in the hybrid hydrodynamic model.

As mentioned before, there is another particle transverse momentum spectra scaling discovered earlier, i.e., Hwa-Yang scaling. They introduced a scaling variable $z = p_{\rm T}/K$, where K is a scaling parameter that depends on both the collision energy and centrality. The scaled spectrum is defined as

$$\Phi(z) = A\frac{1}{2\pi p_{\rm T}}\frac{d^2N}{dp_{\rm T}dy}\bigg|_{z=\frac{p_{\rm T}}{K}}, \tag{28}$$

where A is a normalization factor. By adjusting values of K and A for each particle transverse momentum spectrum, the scaled particle spectra at different energies and centralities all collapse onto the same universal curve $\Phi(z)$. To eliminate the arbitrariness in choosing the reference spectrum, Hwa and Yang further introduced a KNO-like scaling variable $u = z/\langle z\rangle = p_{\rm T}/\langle p_{\rm T}\rangle$, and the corresponding normalized scaling function is defined as

$$\Psi(u) = \frac{\langle z\rangle^2\Phi(\langle z\rangle u)}{\int \Phi(z)zdz}. \tag{29}$$

This function $\Psi(u)$ is independent of both collision energy and centrality, thus providing a universal scaling for the particle spectra from different collision centralities and systems [43–55].

Now we turn to deriving the relation between the scaling found by ExTrEMe Collaboration and the Hwa-Yang scaling. The invariant yield distribution can be rewritten from Eq. (28) as

$$\frac{d^2N}{dp_{\rm T}dy} = \frac{2\pi p_{\rm T}}{A}\Phi(z), \quad z = \frac{p_{\rm T}}{K}. \tag{30}$$

At midrapidity, the rapidity dependence of the particle transverse momentum spectrum is very weak, so one has

$$\frac{dN}{dp_{\rm T}} \approx \Delta y\frac{2\pi p_{\rm T}}{A}\Phi(z). \tag{31}$$

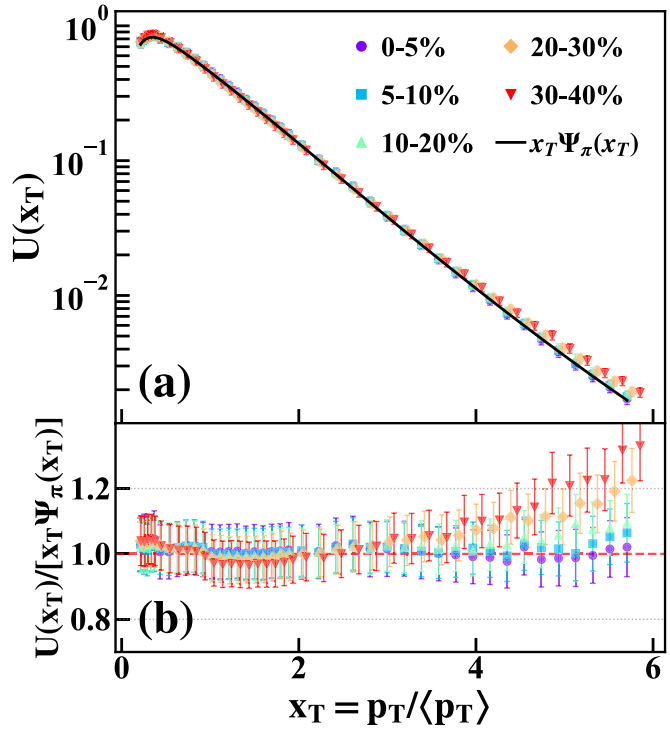


FIG. 5. Panel (a) shows a direct comparison between $U(x_{\rm T})$ (symbols) and $x_{\rm T}\Psi(x_{\rm T})$ (solid curve) for various centrality classes using pion spectra from Pb + Pb collisions at $\sqrt{s_{NN}} = 2.76$ TeV [78]. Panel (b) presents the ratio $R = U(x_{\rm T})/[x_{\rm T}\Psi_\pi(x_{\rm T})]$ for five different centrality bins. The scaling function $\Psi_\pi(x_{\rm T})$ is taken from Ref. [54].

The average total particle multiplicity N for a given particle is then calculated by

$$N = \int_0^\infty \frac{dN}{dp_{\rm T}}dp_{\rm T} = \int_0^\infty \Delta y\frac{2\pi p_{\rm T}}{A}\Phi(z)dp_{\rm T}. \tag{32}$$

Since $p_{\rm T} = Kz$, then $dp_{\rm T} = Kdz$, one has

$$N = \Delta y\frac{2\pi}{A}K^2\int_0^\infty \Phi(z)zdz. \tag{33}$$

It is obvious that

$$\langle p_{\rm T}\rangle = K\langle z\rangle. \tag{34}$$

Substituting Eqs. (31), (33), (34) into the scaled particle transverse momentum spectrum $U(x_{\rm T})$, i.e., Eq. (1), and using the relations $p_{\rm T} = \langle p_{\rm T}\rangle x_{\rm T} = K\langle z\rangle x_{\rm T}$, $z = \langle z\rangle x_{\rm T}$, we obtain

$$\begin{aligned} U(x_{\rm T}) &= \frac{K\langle z\rangle}{K^2\int \Phi(z)zdz}(K\langle z\rangle x_{\rm T})\Phi(\langle z\rangle x_{\rm T}) \\ &= \frac{x_{\rm T}\langle z\rangle^2\Phi(\langle z\rangle x_{\rm T})}{\int \Phi(z)zdz}. \end{aligned} \tag{35}$$

Noting the normalized Hwa-Yang scaling function Eq. (29) and $u = p_{\rm T}/\langle p_{\rm T}\rangle = x_{\rm T}$, we obtain a simple relation

$$U(x_{\rm T}) = x_{\rm T}\Psi(x_{\rm T}). \tag{36}$$

It demonstrates that the two scaling functions are mathematically equivalent, which is another significant contribution of

this work. It is worth noting that the particle transverse momentum spectra scaling found by the ExTrEMe Collaboration has more intuitive physical meaning.

Figure 5 presents a direct comparison of both sides of Eq. (36) using the pion data from Pb + Pb collisions at $\sqrt{s_{NN}} = 2.76$ TeV [78] and the scaling function $\Psi_\pi(x_T)$ obtained in Ref. [54]. Panel (a) displays $U(x_T)$ (symbols) for various centrality classes together with $x_T\Psi_\pi(x_T)$ (curve), while panel (b) shows their ratios. The ratios remain close to unity across all centralities, confirming the relation (36).

V. CONCLUSION

In this paper, we have systematically investigated the scaling properties of the transverse momentum spectra for pions, kaons, and protons in Au + Au collisions from $\sqrt{s_{NN}} = 7.7$ to 200 GeV and in U + U collisions at 193 GeV. Our results demonstrate that the scaled spectra $U(x_T)$ exhibit a centrality-independent shape, confirming that the universality previously observed at the LHC by the ExTrEMe Collaboration extends to the lower energy regime of RHIC. However, a closer examination of the data uncovers characteristic deviations from this ideal scaling. We observe that the scaling breaks down in the high-p_T region and in peripheral collisions, signaling a transition from the hydrodynamic flow regime (soft) to a (semi)hard physics regime. Furthermore, a distinct mass hierarchy is observed. In contrast to pions, which adhere most precisely to the universal curve, kaons and protons show systematically larger deviations in peripheral collisions. This mass-dependent modification is consistent with a reduced radial flow strength in noncentral collisions.

Theoretically, we provide a natural explanation for these phenomena in the framework of a blast-wave-type model built upon the Cooper-Frye formula with certain assumptions. A universal scaling function is derived. We intuitively conjecture that the scaling is strongly relevant to the particle freeze-out mechanism by combining our results and the results from a comprehensive study using the hybrid hydrodynamic models conducted by the ExTrEMe Collaboration [59]. Additionally, we establish the relation between the scaling found by the ExTrEMe Collaboration and the Hwa-Yang scaling, demonstrating that the two scalings are mathematically equivalent. It is interesting to decipher the origin of particle transverse momentum spectra scaling in heavy-ion collisions.

DATA AVAILABILITY

The data that support the findings of this article are openly available [60–64].

[1] *Quark-Gluon Plasma 3*, edited by R. C. Hwa and X. N. Wang (World Scientific, Singapore, 2004).

[2] *Quark-Gluon Plasma 4*, edited by R. C. Hwa and X. N. Wang (World Scientific, Singapore, 2010).

[3] L. P. Csernai, *Introduction to Relativistic Heavy Ion Collisions* (Wiley, New York, 1994).

[4] C. Y. Wong, *Introduction to High-Energy Heavy-Ion Collisions* (World Scientific, Singapore, 1994).

[5] J. Chen *et al.*, Properties of the QCD matter: Review of selected results from the relativistic heavy ion collider beam energy scan (RHIC BES) program, Nucl. Sci. Tech. **35**, 214 (2024).

[6] X. He, S. Shi, and N. Xu, Physics of collectivity and EOS from the RHIC beam energy scan program, Eur. Phys. J. Spec. Top. (2026), doi:10.1140/epjs/s11734-026-02261-7.

[7] Y. Zhang, Z. Wang, X. Luo, and N. Xu, Search for the QCD critical point in high energy nuclear collisions: A status report, Eur. Phys. J. Spec. Top. (2026), doi:10.1140/epjs/s11734-026-02226-w.

[8] S. Mohapatra, Experimental overview on flow observables in heavy ion collisions, Nucl. Phys. A **956**, 59 (2016).

[9] J. Adam *et al.* (ALICE Collaboration), Centrality evolution of the charged–particle pseudorapidity density over a broad pseudorapidity range in Pb–Pb collisions at $\sqrt{s_{\rm NN}} = 2.76$ TeV, Phys. Lett. B **754**, 373 (2016).

[10] B. I. Abelev *et al.* (STAR Collaboration), Rapidity and species dependence of particle production at large transverse momentum for d + Au collisions at $\sqrt{s_{NN}} = 200$ GeV, Phys. Rev. C **76**, 054903 (2007).

[11] J. Q. Tao, M. Wang, H. Zheng, W. C. Zhang, L. L. Zhu, and A. Bonasera, Pseudorapidity distributions of charged particles in pp($\bar{\rm p}$), p(d)A and AA collisions using Tsallis thermodynamics, J. Phys. G **48**, 105102 (2021).

[12] J. Tao, H. He, H. Zheng, W. Zhang, X. Liu, L. Zhu, and A. Bonasera, Pseudo-rapidity distributions of charged particles in asymmetric collisions using Tsallis thermodynamics, Nucl. Sci. Tech. **34**, 172 (2023).

[13] W. Zhao, L. Zhu, H. Zheng, C. M. Ko, and H. Song, Spectra and flow of light nuclei in relativistic heavy ion collisions at energies available at the BNL relativistic heavy ion collider and at the CERN large hadron collider, Phys. Rev. C **98**, 054905 (2018).

[14] Z.-G. Tan, S.-J. Wang, Y.-N. Guo, H. Zheng, and A. Bonasera, A novel encoding mechanism for particle physics, Nucl. Sci. Tech. **35**, 144 (2024).

[15] S. Jena and R. Gupta, A unified formalism to study transverse momentum spectra in heavy-ion collision, Phys. Lett. B **807**, 135551 (2020).

[16] R. J. Fries, B. Muller, C. Nonaka, and S. A. Bass, Hadronization in heavy ion collisions: Recombination and fragmentation of partons, Phys. Rev. Lett. **90**, 202303 (2003).

[17] J. Adams *et al.* (STAR Collaboration), Multistrange baryon production in Au-Au collisions at $\sqrt{s_{NN}} = 130$ GeV, Phys. Rev. Lett. **92**, 182301 (2004).

[18] R. Gupta, A. Menon, S. Jain, and S. Jena, The theoretical description of the transverse momentum spectra: A unified model, Universe **9**, 111 (2023).

[19] J. Tao, W. Wu, M. Wang, H. Zheng, W. Zhang, L. Zhu, and A. Bonasera, The novel scaling of Tsallis parameters from the transverse momentum spectra of charged particles in heavy-ion collisions, Particles **5**, 146 (2022).

[20] Z. Xie, A. K. Lei, H. Zheng, W. C. Zhang, D. M. Zhou, Z. L. She, Y. L. Yan, and B. H. Sa, Particle productions in $p\bar{p}$ collisions in the PACIAE 4.0 model, arXiv:2603.12007.

[21] M. A. C. Lamont, Investigation of the high-p_T strange baryon anomalies at RHIC, Eur. Phys. J. C **49**, 35 (2007).

[22] A. Adare *et al.* (PHENIX Collaboration), Spectra and ratios of identified particles in Au+Au and d + Au collisions at $\sqrt{s_{NN}}$ = 200 GeV, Phys. Rev. C **88**, 024906 (2013).

[23] B. B. Abelev *et al.* (ALICE Collaboration), Production of charged pions, kaons and protons at large transverse momenta in pp and Pb–Pb collisions at $\sqrt{s_{\rm NN}}$ = 2.76 TeV, Phys. Lett. B **736**, 196 (2014).

[24] K. Adcox *et al.* (PHENIX Collaboration), Suppression of hadrons with large transverse momentum in central Au+Au collisions at $\sqrt{s_{NN}}$ = 130 GeV, Phys. Rev. Lett. **88**, 022301 (2001).

[25] J. Adams *et al.* (STAR Collaboration), Evidence from d + Au measurements for final state suppression of high p_T hadrons in Au+Au collisions at RHIC, Phys. Rev. Lett. **91**, 072304 (2003).

[26] M. Csanad *et al.*, Universal scaling of the elliptic flow data at RHIC, Eur. Phys. J. A **38**, 363 (2008).

[27] M. Wang, J.-Q. Tao, H. Zheng, W.-C. Zhang, L.-L. Zhu, and A. Bonasera, Number-of-constituent-quark scaling of elliptic flow: A quantitative study, Nucl. Sci. Tech. **33**, 37 (2022).

[28] L. Adamczyk *et al.* (STAR Collaboration), Centrality and transverse momentum dependence of elliptic flow of multi-strange hadrons and ϕ meson in Au+Au collisions at $\sqrt{s_{NN}}$ = 200 GeV, Phys. Rev. Lett. **116**, 062301 (2016).

[29] J. Adams *et al.* (STAR Collaboration), Azimuthal anisotropy in Au+Au collisions at $\sqrt{s_{NN}}$ = 200 GeV, Phys. Rev. C **72**, 014904 (2005).

[30] C. Adler *et al.* (STAR Collaboration), Elliptic flow from two and four particle correlations in Au+Au collisions at $\sqrt{s_{\rm NN}}$ = 130 GeV, Phys. Rev. C **66**, 034904 (2002).

[31] Z. Koba, H. B. Nielsen, and P. Olesen, Scaling of multiplicity distributions in high-energy hadron collisions, Nucl. Phys. B **40**, 317 (1972).

[32] I. Sarcevic, KNO scaling in hadron-hadron collisions, Acta Phys. Pol. B **19**, 361 (1988).

[33] X.-P. Duan, L. Chen, G.-L. Ma, C. A. Salgado, and B. Wu, Koba-Nielsen-Olesen scaling in quark and gluon jets at the LHC, Phys. Rev. D **112**, 094022 (2025).

[34] J. D. Bjorken, Asymptotic sum rules at infinite momentum, Phys. Rev. **179**, 1547 (1969).

[35] G. Altarelli and G. Parisi, Asymptotic freedom in parton language, Nucl. Phys. B **126**, 298 (1977).

[36] T. Regge, Introduction to complex orbital momenta, Nuovo Cim. **14**, 951 (1959).

[37] A. R. White, Analytic multi - Regge theory and the pomeron in QCD II: Gauge theory analysis, Int. J. Mod. Phys. A **8**, 4755 (1993).

[38] M. A. Braun, E. M. Kuzminskii, and M. I. Vyazovsky, On the Reggeon model with the pomeron and odderon: Singularities with non-zero masses, Eur. Phys. J. C **85**, 1415 (2025).

[39] R. P. Feynman, Very high-energy collisions of hadrons, Phys. Rev. Lett. **23**, 1415 (1969).

[40] J. Benecke, T. T. Chou, C.-N. Yang, and E. Yen, Hypothesis of limiting fragmentation in high-energy collisions, Phys. Rev. **188**, 2159 (1969).

[41] G. H. Arakelyan, C. Merino, C. Pajares, and Y. M. Shabelski, Feynman scaling violation on baryon spectra in *pp* collisions at LHC and cosmic ray energies, Phys. At. Nucl. **76**, 316 (2013).

[42] K. Jiang, Y. Zhu, W. Liu, H. Chen, C. Li, L. Ruan, Z. Tang, and Z. Xu, Onset of radial flow in $p + p$ collisions, Phys. Rev. C **91**, 024910 (2015).

[43] R. C. Hwa and C. B. Yang, Scaling behavior at high p_T and the p/π ratio, Phys. Rev. C **67**, 034902 (2003).

[44] R. C. Hwa and C. B. Yang, Centrality scaling of the p_T distribution of pions, Phys. Rev. Lett. **90**, 212301 (2003).

[45] R. C. Hwa and C. B. Yang, Scaling distributions of quarks, mesons and proton for all p_T, energy and centrality, Phys. Rev. C **67**, 064902 (2003).

[46] L. L. Zhu and C. B. Yang, Universal scaling of p_T distribution of particles in relativistic nuclear collisions, Phys. Rev. C **75**, 044904 (2007).

[47] Zheng Fang-Lan and Yang Chun-Bin, Scaling p_T distribution in small rapidity region and pseudorapidity asymmetry for charged hadron in d + Au collisions at $\sqrt{s_{NN}}$ = 200 GeV, Commun. Theor. Phys. **49**, 1580 (2008).

[48] L. L. Zhu, H. Zheng, and C. B. Yang, Scaling and multiplicity dependence of p_T spectra in *pp* collisions at $\sqrt{s_{NN}}$ = 200 GeV, Nucl. Phys. A **809**, 259 (2008).

[49] L. L. Zhu, H. Zheng, and C. B. Yang, Scaling behavior of transverse kinetic energy distributions in Au+Au collisions at $\sqrt{s_{NN}}$ = 200 GeV, Nucl. Phys. A **802**, 122 (2008).

[50] W. C. Zhang, Y. Zeng, W. X. Nie, L. L. Zhu, and C. B. Yang, Scaling of p_T distributions for p and $\bar{p}$ produced in Au + Au collisions at $\sqrt{s_{NN}}$ = 200 GeV, Phys. Rev. C **76**, 044910 (2007).

[51] W. C. Zhang and C. B. Yang, Scaling behavior of charged hadron p_T distributions in pp and p$\bar{\rm p}$ collisions, J. Phys. G **41**, 105006 (2014).

[52] W. C. Zhang, Scaling behaviours of the p_T spectra for identified hadrons in *pp* collisions, J. Phys. G **43**, 015003 (2016).

[53] L. Yang, Y. Wang, W. Hao, N. Liu, X. Du, and W. Zhang, Universal scaling of strange particle p_T spectra in pp collisions, Eur. Phys. J. A **54**, 54 (2018).

[54] Y. Wang, L. Yang, X. Du, N. Liu, L. Qiao, and W. Zhang, Universal scaling of the pion, kaon and proton p_T spectra in Pb-Pb collisions at 2.76 TeV, Nucl. Phys. A **976**, 46 (2018).

[55] N. Liu, X. Du, L. Qiao, G. Che, and W. Zhang, Universal scaling of meson and baryon spectra in p-Pb collisions at 5.02 TeV, Int. J. Mod. Phys. E **28**, 1950030 (2019).

[56] C. D. Muncinelli, F. G. Gardim, D. D. Chinellato, G. S. Denicol, A. V. Giannini, M. Luzum, J. Noronha, T. N. da Silva, J. Takahashi, and G. Torrieri (ExTrEMe Collaboration), Universality of scaled particle spectra in ultrarelativistic heavy-ion collisions, Phys. Rev. C **112**, 064922 (2025).

[57] T. S. Domingues *et al.*, Probing the onset of collectivity via scaled particle spectra in ultrarelativistic nuclear collisions, EPJ Web of Conferences **364**, 04011 (2026).

[58] T. S. Domingues and M. Luzum, Scaled transverse-momentum spectra as a probe of collective dynamics in heavy-ion collisions, arXiv:2603.15891.

[59] T. S. Domingues *et al.*, The shape of transverse momentum spectra in hybrid hydrodynamic models, arXiv:2602.22490.

[60] L. Adamczyk *et al.* (STAR Collaboration), Bulk properties of the medium produced in relativistic heavy-ion collisions from the beam energy scan program, Phys. Rev. C **96**, 044904 (2017).

[61] J. Adam *et al.* (STAR Collaboration), Bulk properties of the system formed in Au + Au collisions at $\sqrt{s_{NN}}$ = 14.5 GeV at the BNL STAR detector, Phys. Rev. C **101**, 024905 (2020).

[62] B. I. Abelev *et al.* (STAR Collaboration), Energy dependence of $\pi^{\pm}$, p, and $\bar{p}$ transverse momentum spectra for Au+Au collisions at $\sqrt{s_{\rm NN}} = 62.4$ and 200 GeV, Phys. Lett. B **655**, 104 (2007).

[63] S. S. Adler *et al.* (PHENIX Collaboration), Identified charged particle spectra and yields in Au+Au collisions at $\sqrt{s_{NN}} = 200$ GeV, Phys. Rev. C **69**, 034909 (2004).

[64] M. S. Abdallah *et al.* (STAR Collaboration), Pion, kaon, and (anti)proton production in U+U collisions at $\sqrt{s_{NN}} = 193$ GeV measured with the STAR detector, Phys. Rev. C **107**, 024901 (2023).

[65] R. Bashir, R. Shehzadi, M. U. Ashraf, and A. M. Khan, Predictions for identified hadron ($\pi^{\pm}$, $K^{\pm}$, and $p(\overline{p})$) production and collective dynamics in oxygen–oxygen collisions at $\sqrt{s_{NN}} = 7$ TeV with EPOS4, AMPT-SM, and Angantyr in PYTHIA 8, Eur. Phys. J. Plus **140**, 1211 (2025).

[66] C. Gale, S. Jeon, and B. Schenke, Hydrodynamic modeling of heavy-ion collisions, Int. J. Mod. Phys. A **28**, 1340011 (2013).

[67] W. Florkowski, M. P. Heller, and M. Spalinski, New theories of relativistic hydrodynamics in the LHC era, Rep. Prog. Phys. **81**, 046001 (2018).

[68] B. I. Abelev *et al.* (STAR Collaboration), Centrality dependence of charged hadron and strange hadron elliptic flow from $\sqrt{s_{NN}} = 200$ GeV Au + Au collisions, Phys. Rev. C **77**, 054901 (2008).

[69] J.-H. Shi, Z.-Y. Qin, J.-P. Zhang, J. Cao, Z.-F. Jiang, W.-C. Zhang, and H. Zheng, Nonextensive (3+1)-dimensional hydrodynamics for relativistic heavy-ion collisions, Phys. Rev. D **111**, 036010 (2025).

[70] L.-G. Pang, H. Petersen, and X.-N. Wang, Pseudorapidity distribution and decorrelation of anisotropic flow within the open-computing-language implementation CLVisc hydrodynamics, Phys. Rev. C **97**, 064918 (2018).

[71] F. Cooper and G. Frye, Comment on the single particle distribution in the hydrodynamic and statistical thermodynamic models of multiparticle production, Phys. Rev. D **10**, 186 (1974).

[72] F. Becattini, V. Chandra, L. Del Zanna, and E. Grossi, Relativistic distribution function for particles with spin at local thermodynamical equilibrium, Ann. Phys. **338**, 32 (2013).

[73] K. Ürmössy and T. S. Biro, Cooper-Frye formula and nonextensive coalescence at RHIC energy, Phys. Lett. B **689**, 14 (2010).

[74] G. Che, J. Gu, W. Zhang, and H. Zheng, Identified particle spectra in Pb–Pb, Xe–Xe and p–Pb collisions with the Tsallis blast-wave model, J. Phys. G **48**, 095103 (2021).

[75] F. Retiere and M. A. Lisa, Observable implications of geometrical and dynamical aspects of freeze out in heavy ion collisions, Phys. Rev. C **70**, 044907 (2004).

[76] W. Florkowski and W. Broniowski, Hydro-inspired parameterizations of freeze-out in relativistic heavy-ion collisions, Acta Phys. Pol. B **35**, 2895 (2004).

[77] E. Schnedermann, J. Sollfrank, and U. W. Heinz, Thermal phenomenology of hadrons from 200*A* GeV S+S collisions, Phys. Rev. C **48**, 2462 (1993).

[78] B. Abelev *et al.* (ALICE Collaboration), Centrality determination of Pb-Pb collisions at $\sqrt{s_{NN}} = 2.76$ TeV with ALICE, Phys. Rev. C **88**, 044909 (2013).